RSC Advances

Modeling of Biosynthesized Silver Nanoparticles in *Vitex Negundo* L. Extract by Artificial Neural Network

Parvaneh Shabanzadeh [1, 2], Rubiyah Yusof [1, 2,] *, Kamyar Shameli [2]

[1]Centre for Artificial Intelligence and Robotics, Universiti Teknologi Malaysia, 54100 Kuala Lumpur, Malaysia

[2]Malaysia-Japan International Institute of Technology (MJIIT), Universiti Teknologi Malaysia, Jalan Sultan Yahya Petra (Jalan Semarak), 54100 Kuala Lumpur, Malaysia

*Corresponding author: rubiyah.kl@utm.my

Tel: +60173371365

Abstract

In this study silver nanoparticles (Ag-NPs) are biosynthesized from silver nitrate aqueous solution through a simple and eco-friendly route using water extract of *Vitex negundo* L. (*V. negundo*) which acted as a reductant and stabilizer simultaneously. The as prepared samples are characterized using UV–visible spectroscopy, X-ray diffraction (XRD), and transmission electron microscopy (TEM). Also artificial neural network (ANN) model was presented for synthesized silver nanoparticles in *V. negundo* L. extract. The aim was to predict size of silver nanoparticles produced as a function of the weight percentage of *V. negundo* L. extract, reaction of temperature, stirring time and molar concentration of $AgNO_3$. The fast Levenberg–Marquardt (LM) optimization technique was employed for training of ANN model. The optimized ANN was as a multilayer perceptron (MLP) network with two hidden layers and 10 neurons. Therefore ANN is found out to be an efficient tool to model the complicated chemical field. This model is capable for predicting the size of nanoparticles for a wide range of conditions with a mean square error 0.4576 and a regression of about 0.998. Based on the presented model it is possible to design an effective green method for obtain silver nanoparticles, while minimum received materials are used and minimum size of nanoparticles will be obtained.

Keywords: Modeling, artificial neural network, *Vitex negundo*, silver nanoparticles.

Introduction

The field of nanotechnology is one of the most active areas of research in modern material science. Nanoparticles exhibit completely new or improved properties based on specific characteristics such as size, distribution and morphology. The crystal silver nanoparticles have found tremendous applications in the field of high sensitivity biomolecular detection and diagnostics, antimicrobials and therapeutics, catalysis and micro-electronics.

A number of approaches are available for the synthesis of silver nanoparticles for example, reduction in solutions, chemical and photochemical reactions in reverse micelles, thermal decomposition of silver compounds, radiation assisted, electrochemical, sonochemical, microwave assisted process and recently via green biosynthetic route [1].

The biosynthesis of nanoparticles, which represents a connection between biotechnology and nanotechnology, has received increasing consideration due to the growing need to develop environmentally friendly technologies for material syntheses. The search for appropriate biomaterials for the biosynthesis of nanoparticles continues through many different synthetic methods [2]. The biosynthetic method using plant extracts has received more attention than chemical and physical methods and even than the use of microbes. The method is suitable for nanoscale metal synthesis due to the absence of any requirement to maintain an aseptic environment [3]. The possibility of using plant materials for the synthesis of nanoscale metals was reported initially by Gardea-Torresdey et al. [4, 5].

In continuation, we have demonstrated the prospect of using *Curcuma longa* tuber powder water extract, *Callicarpa manigayi* stem bark and *V. negundo L.* methanolic extracts for the synthesis of the Ag-NPs [6-9].

Basically, Artificial Neural Networks were inspired by the learning process in the human brain. Since 1940 till now, it has been evolved steadily and was adopted in many areas of science and various fields such as process control, pattern recognition, forecasting, and system identification [10-12]. In recent years, ANNs have been used as a powerful modeling tool in various chemical processes such as [13-15].

In the ANN modeling approach, it requires known input data set without any assumptions; therefore it has several advantages over traditional mathematical or statistical models. In order to predict the desired output as a function of suitable inputs, ANN develops a mapping of the input into output variables. Almost more of multilayer neural networks by selecting a suitable set of connecting weights and transfer functions can approximate any smooth, measurable function between input and output vectors [16-18]. The objective of this paper is to reach the prediction model to the evaluate influence of different variables on size of silver nanoparticles obtained by *V. negundo* L. extract and compression the experimental data with predicted neural network model's values.

2. Materials and Methods

2.1. Materials

Mature leaves of *V. negundo* were collected from the University Agriculture Park, and Herbal unit at University Putra Malaysia (UPM). $AgNO_3$ (99.98%), methanol (CH_3OH, 99.9%), nutrient agar and Muller Hinton agar were purchased from Merck (Germany). All aqueous solutions were prepared using double distilled water. All reagents were of analytical grade.

2.2. Extract Preparation

The *V. negundo* green leaves were washed and dried utilizing oven dryer at 40 ºC for 48 h. The dried leaves were then ground into powder, stored in dark glass bottles and kept at –20 °C until further analyses. The finely ground *V. negundo* leaves were extracted with methanol (ratio 1:10 w/v) using a shaking water bath for overnight at 40 ºC. After filtration with Whatman filter paper No 1 using vacuum pump, the residue was re-extracted again. The solvent was completely removed using a rotary vacuum evaporator (Buchi, Flavil, Switzerland) at 40 °C. The concentrated extracts were kept in dark bottles at 4 °C until used.

2.3. Synthesis of Ag/*V. Negundo* Emulsion

In a typical reaction procedure, 0.5 g crude extract of *V. negundo* was added to 100 ml distilled de-ionized water with vigorous stirring for 1 hr, then 100 ml $AgNO_3$ (1×10^{-1} M) was added and mixed at room temperature for 1, 3, 6, 24, and 48 h. The Ag-NPs were gradually obtained during the incubation period.

2.4. Characterization methods and instruments

The synthesized Ag/*V. negundo* were characterized using Ultraviolet-visible (UV-vis) spectroscopy, X-ray diffraction (XRD) and transmission electron microscopy (TEM). Meanwhile, the structures of the Ag-NPs were studied using the X-ray diffraction (XRD, Philips, X'pert, Cu Kα) at a scanning speed of 4°/min. TEM images were obtained with a Hitachi H-

7100® electron microscope (Hitachi High-Technologies Corporation, Tokyo, Japan), and the mean particle size distributions of nanoparticles were determined using the UTHSCSA Image Tool® Version 3.00 program (UTHSCSA Dental Diagnostic Science, San Antonio, TX, USA). The UV–vis spectra were recorded over the range of 300–700 nm with an H.UV 1650 PC-SHIMADZU B, UV-vis spectrophotometer.

2.5. Artificial Neural Network

The ANN is an information processing system that is inspired by the way such as biological nervous systems e.g. brain [19]. The purpose of an ANN is to calculate output values from input values by black box computations. The basic part of a neural network is the neuron, also called “node”. Neural networks are made of several neurons that perform in parallel or in sequence. In Figure 1 is illustrated a single node of a neural network. Inputs of network are shown as $\mathrm{I_i}$ and the output as Y. An artificial neural network can has many inputs and output signals. The intensity of the input signals in the network, are determined by especial coefficients "weight" s that presented as $\mathrm{W_i}$. The outs of nods are obtained by using transfer functions, so that they transform the inputs of nods in a linear or nonlinear manner. Three types of commonly used transfer functions are as follows:

• Linear transfer function

$$\mathrm{f(x) = x}\,,\quad -\infty \le \mathrm{f(x)} \le +\infty \qquad (1)$$

• Sigmoid transfer function

$$\mathrm{f(x)} = 1/(1 + \mathrm{e^{-x}})\,,\quad 0 \le \mathrm{f(x)} \le 1 \qquad (2)$$

• Hyperbolic tangent transfer function

$$\mathrm{f(x)} = (\mathrm{e^{x}} - \mathrm{e^{-x}})/(\mathrm{e^{x}} + \mathrm{e^{-x}}),\quad -1 \le \mathrm{f(x)} \le 1 \qquad (3)$$

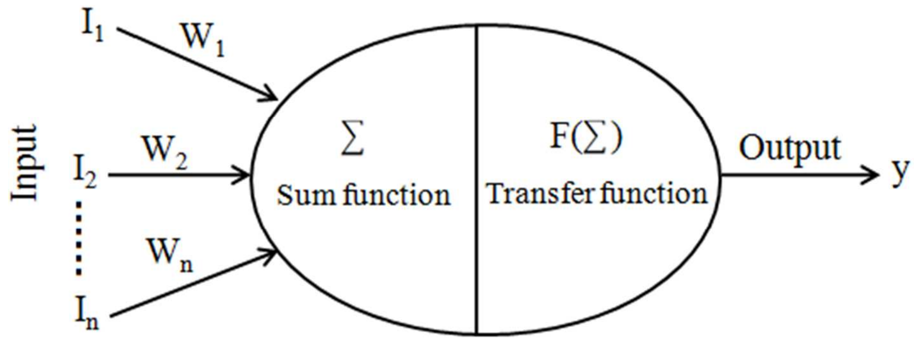

Figure 1. Artificial neural network: operation of a single neuron.

ANN training process is an optimization process the which takes a set of input dataset and checks the output for the desired output by systematically adjusting of weights so that the network can predict the correct outputs. The training process modifies the weight and biases until the accuracy of results prediction be acceptable, then the ANN learns how to predict. One of the most common algorithms for training process is the feed forward back propagation (FFBP) neural network [20], which is a multiple-layer network with an input layer, an output layer and some hidden layers between the input and output layers [21]. Different types of algorithm of training with mathematical aspects of them are comprehensively described in the literature [22-25].

The input–output relationship between each node of a hidden layer can be written as follows

$$\alpha j = f\left(\sum_{i=1}^{j}(W_{ji}P_i) + b_j\right) \quad (4)$$

Where αj is the output from the j th node of the previous layer and f is a transfer function. The W_{ji} is the weight of the connection between the i th node and the current node, and b_j is the bias of the current node.

The most widely criteria used for evaluation of the performance of the ANN model are the mean squared error (MSE) and correlation coefficient (R). In statistics, R indicates the strength and direction of a linear relationship between two variables. In general statistical usage R refers to the departure of two variables from independence. A number of different coefficients are used for different situations. The iteration of leaning process terminates when MSE of performance is less than a specific tolerance (here, 10^{-3}). The MSE and R are as follow:

$$MSE = \left(\sum_{i\epsilon N}(YO_i - Y_i)^2\right)/N \quad (5)$$

$$R^2 = 1 - \frac{\sum_{i\epsilon N}(YO_i - Y_i)^2}{\sum_{i\epsilon N}(Y_i - \bar{Y})^2} \tag{6}$$

Where YO_i, Y_i respectively represents the output and observed values, $\bar{Y}$ is average of the observed values and N is the total number of data points.

3. Results and Discussion

3.1. UV-vis Spectroscopy Analysis

Reduction of Ag^+ into Ag-NPs during exposure to water extract of *V. negundo* could be followed by the color change. The fresh suspension of *V. negundo* was yellow in color [Figure 2 (a)]. After addition of $AgNO_3$ and change the condition of reaction the emulsion turned to brown color [Figure 2 (b)].

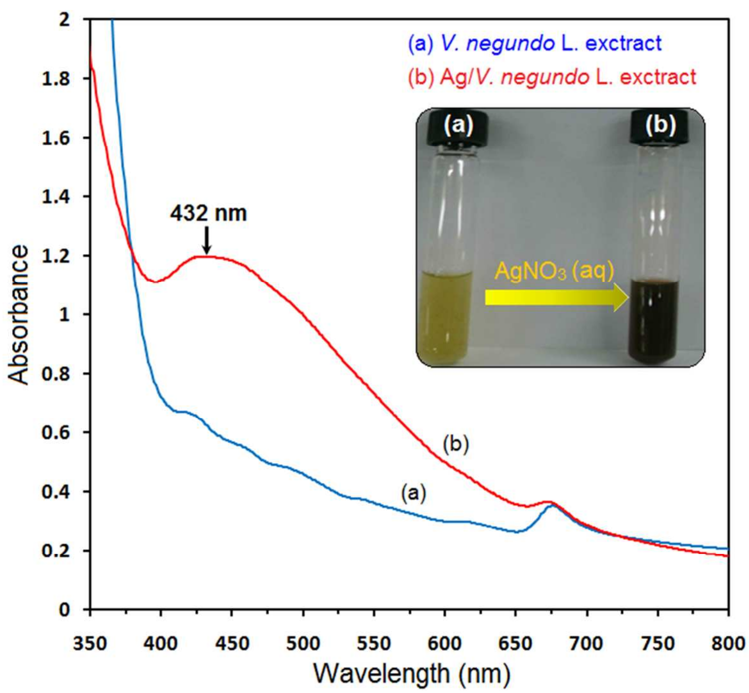

Figure 2. UV–vis absorption spectra and photographs of (a) *V. negundo* aqueous extract and (b) Ag/*V. negundo* emulsion.

The preparation of Ag-NPs was studied by UV-vis spectroscopy, which has proven to be a useful spectroscopic method for the detection of prepared metallic nanoparticles. The formation of Ag-NPs was followed by measuring the surface plasmon resonance of the *V. negundo* and Ag/*V. negundo* emulsions over the wavelength range from 300 to 800 nm. Figure 2 shows that

Ag-NPs started forming when $AgNO_3$ reacted directly with *V. negundo* at a room temperature. In UV-vis spectra, the spherical Ag-NPs must display a surface plasmon resonance band at around 400–450 nm [26].

3.2. X-ray Diffraction

Figure3 shows the X-ray diffraction (XRD) patterns of vacuum-dried Ag-NPs synthesized using *V. negundo*. The XRD patterns of Ag/*V. negundo* indicated that the structure of Ag-NPs is face-centered cubic (fcc).

In addition, all the Ag-NPs had a similar diffraction profile and XRD peaks at 2θ of 38.17°, 44.413°, 64.44°, 77.37° and 81.33° could be attributed to the 111, 200, 220, 311 and 222 crystallographic planes of the face-centered cubic (fcc) silver crystals, respectively [27]. The XRD pattern thus clearly illustrated that the Ag-NPs formed in this study are crystalline in nature. The main crystalline phase was silver and there was no obvious other phases as impurities were found in the XRD patterns (Ag XRD Ref. No. 01-087-0719).

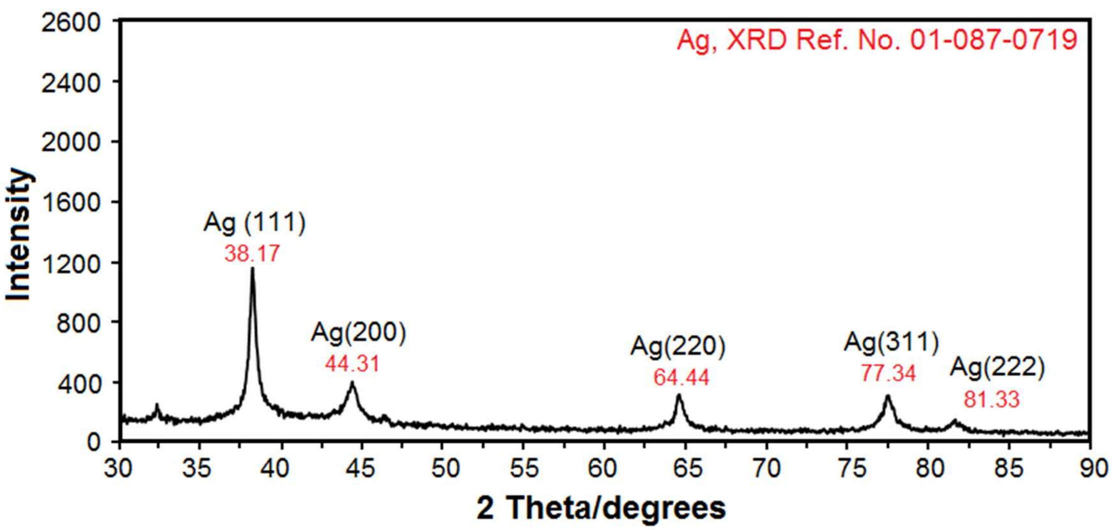

Figure 3. XRD patterns of Ag-NPs synthesized in *V. negundo* aqueous extract.

3.3. Morphology study

TEM image and their corresponding particle size distributions of Ag-NPs on *V. negundo* L. extract are shown in Figure 4 (a) and (b). For the TEM study, drops of the Ag-NPs solutions synthesized was deposited onto a TEM copper grid. After drying, the grid was imaged using TEM. The TEM image and their size distribution revealed that, the mean diameter of Ag-NPs was less than 30 nm. There are can be observed clearly that Ag-NPs surrounded by the *V. negundo* extract in the high magnification of TEM. Thus, these results confirm that extract of *V. negundo* can control shape and size of the Ag NPs. This result approved that the size of the synthesized Ag-NPs depended to reaction stirring time, temperature, *V. negundo* extract and $AgNO_3$ concentration.

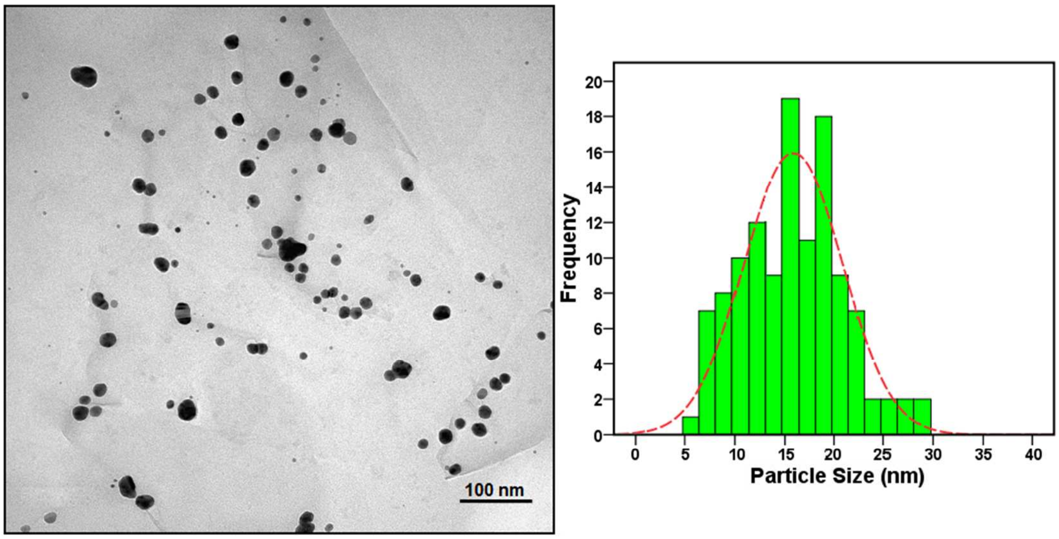

Figure 4. TEM image and corresponding size distribution of Ag-NPs in *V. negundo* extract.

3.4. Computational models

The neural network model was implemented in MATLAB, in which technique is available in the Neural Network Toolbox. The inputs of data for ANN modeling were the *V. negundo* extract, stirring time, Temperature of reaction and $AgNO_3$ concentration of 30 prepared samples, while the output data was the size of nano particles.

It should be attention that the range of input variables was dissimilar. Therefore, each of input variables was normalized in the range of -1 to 1 by the following equation:

$$xn_i = \frac{(x_i - \mathrm{minX})}{(\mathrm{maxX} - \mathrm{minX})} * 2 - 1 \qquad i = 1, \ldots, \dim(X) \qquad (7)$$

where xn_i denotes ith normalized input of (X), x_i is ith input variable of X, and minX and maxX show minimum and maximum of input variable of X, as respective.

The experimental divided into three sections (train, test, and validation) due to avoiding over fitting [28]. This method is called "early stopping" that is used to protect network from over fitting [29, 30]. The train dataset is always used to training of the network model while validation dataset is applied to determine the optimum network architecture and also to stop training network when over learning takes placed. The test dataset is just applied to evaluate the network. Also “The test set was utilized to avoid over fitting by controlling errors" [31]. It must be mentioned that validation and test data were not used in training of ANN model.

The optimal ANN architecture was found with four neurons (the *V. negundo* extract, stirring time, temperature of reaction and $AgNO_3$ concentration), one neuron (size of nanoparticles) and 10 neurons in the hidden layer as 4:10:1, with the hyperbolic tangent and the pure line transfer functions for hidden and output layers, respectively (Figure 5), while the weight and bias values of each layer were determined.

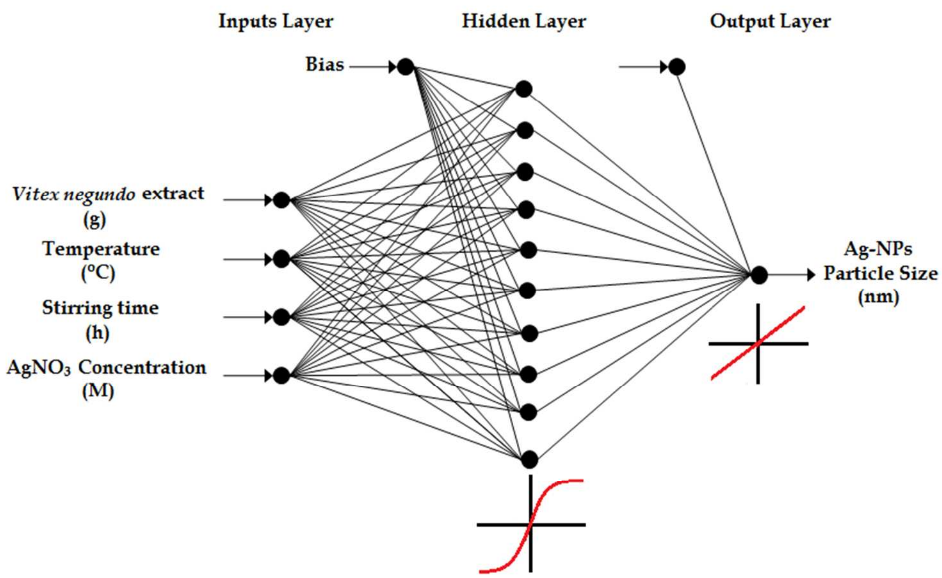

Figure 5. The optimums ANN model for prediction the size of Ag-NPs in *V. negundo* L. extract.

In Table 1 is presented the experimental data used for the obtaining of best ANN model. The predicted particle size is compared to the observed particle size and the difference between the predicted and observed size is stated as particle size error based on the difference between these two values.

Table 1. Experimental values (train, validation, and test data set), actual and model predicated of size of Ag-NPs.

Run No	Plant Extract in 100 water (g)	Temperature of Reaction (C)	Stirring Time (hour)	Molar Concentration of 100 (mL) $AgNO_3$	Size of Silver (Actual) (nm)	Size of Silver (Predict) (nm)	Error= Actual-Predict (nm)
1	0.1	25	48	0.1	27.39	28.383	-0.99308
2	0.1	30	48	0.2	28.44	28.737	-0.29705
3	0.1	40	48	0.5	28.83	28.84	-0.0104
4	0.1	50	48	1	29.31	29.313	-0.00334
5	0.1	60	48	1.5	30.98	30.927	0.052567
6	0.1	70	24	2	31.79	30.443	1.3466
7	0.25	25	24	0.1	24.62	24.637	-0.01667
8	0.25	30	24	0.2	25.77	25.787	-0.01734
9	0.25	40	24	0.5	26.08	26.101	-0.02101
10	0.25	50	24	1	26.84	26.223	0.61658
11	0.25	60	12	1.5	27.49	27.483	0.007177
12	0.25	70	12	2	28.53	28.489	0.040549
13	0.5	25	12	0.1	18.23	18.059	0.17082
14	0.5	30	12	0.2	19.21	19.125	0.084778
15	0.5	40	12	0.5	20.67	21.099	-0.42885
16	0.5	50	6	1	21.32	21.355	-0.03466
17	0.5	60	6	1.5	23.78	23.809	-0.02877
18	0.5	70	6	2	24.12	24.157	-0.03654
19	0.75	25	6	0.1	15.37	15.425	-0.05481
20	0.75	30	6	0.2	16.43	16.769	-0.33903
21	0.75	40	3	0.5	17.83	17.882	-0.05204
22	0.75	50	3	1	19.33	18.772	0.55796
23	0.75	60	3	1.5	19.85	19.884	-0.03443
24	0.75	70	3	2	20.74	20.33	0.41021
25	1	25	3	0.1	15.64	15.664	-0.02369
26	1	30	1	0.2	16.44	16.484	-0.04385
27	1	40	1	0.5	17.31	17.358	-0.04816
28	1	50	1	1	17.55	17.58	-0.02975
29	1	60	1	1.5	18.47	18.488	-0.01838
30	1	70	1	2	18.72	18.74	-0.02016

In the Table 2 is shown the values of connection weights (parameters of the model) for the complete ANN model trained on the experimental datasets. This information let other researchers can use present ANN model with their own experimental data.

Table 2. Values of connection weights and biases for the proposed ANN model.

	Node1	Node2	Node3	Node4	Node5	Node6	Node7	Node8	Node9	Node10	Bias 2
Input 1	1.2888	0.80109	-1.4691	0.4282	0.17815	-1.8229	-1.8128	-0.4232	2.5278	1.5863	
Input 2	-1.4193	1.8848	2.1709	-0.24801	0.44858	-1.525	-0.21333	2.3386	0.8617	1.5071	
Input 3	0.86468	-1.359	1.6485	0.82539	0.78086	0.17248	1.1837	0.13042	1.1185	-1.1452	
Input 4	1.1096	-0.68414	-1.1089	-2.0553	-2.7909	1.2445	1.3834	-1.0763	1.1503	-1.1424	
Output	-0.1686	-0.19511	0.43103	0.1953	-0.24939	0.2941	-0.12225	0.37159	0.20407	-0.15654	
Bias 1	-2.6573	-1.6986	0.60093	-0.1745	0.35521	-0.3558	0.043435	1.5129	1.2438	2.1805	-0.4754

As mentioned in [30,32-34], the error functions (R and MSE are carried out based on predicted output and actual output) are commonly used and applied for evaluation and presentation of every statistical or mathematical model. The values of MSE and R for the optimum architecture were presented in table3. Therefore they were employed in our work that which as clearly show power and accuracy of optimized ANN model. Then the results showed that the network can predict the unused date with high accuracy.

Table 3. The performances of ANN model on train, validation and test data sets.

Test	R	MSE
Train	1.0000	0.0011
Validation	0.9938	0.359
Test	0.9982	0.4576

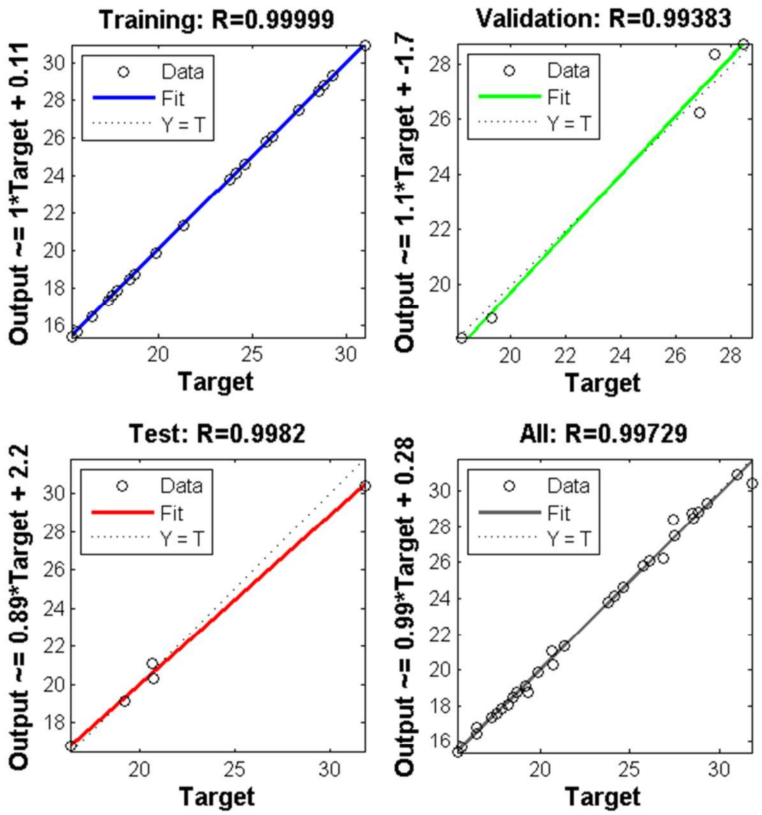

Figure 6. The scatter plots of ANN model for train, validation, test and all data sets.

Also, in the Figure 6 is shown the scatter diagram of predicted values by ANN modeling (Output) in comparison with experimental values (Target). It is indicating good predictive ability of the proposed model is obtained by the ANN process [38].

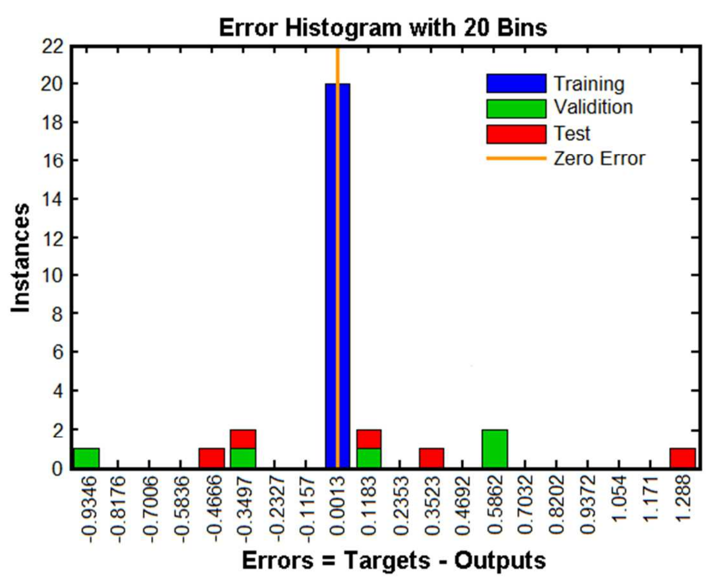

Figure 7. Error histogram of train, validation, and test datasets.

In the Figure 7 is shown the errors histogram of train, validation and test sets. These results specify that the experimental data has been fitted with proper accuracy using the obtained ANN model.

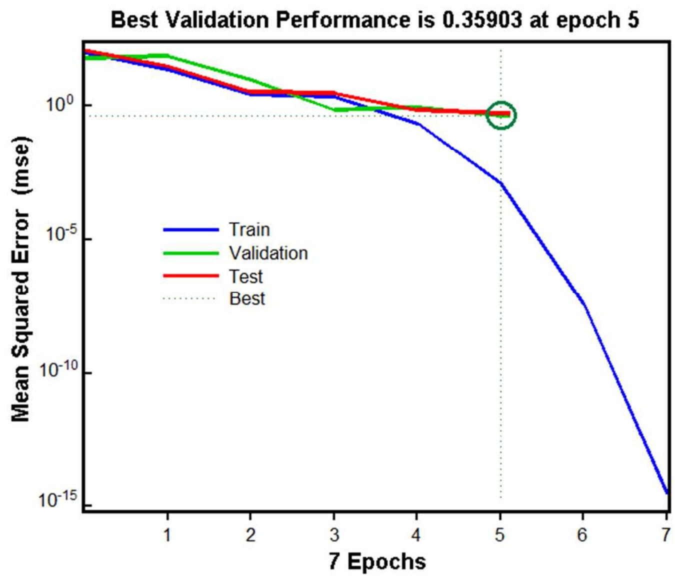

Figure 8. Mean squared error of experimental datasets. (train, validation, and test)

Figure 8 represents the MSE of test, train, and validation datasets for 5 iterations, and the best validation performance is found to in 0.359 in the 5th epoch (iteration). The results of Figure 8 show other reasons for validating the final obtained ANN model.

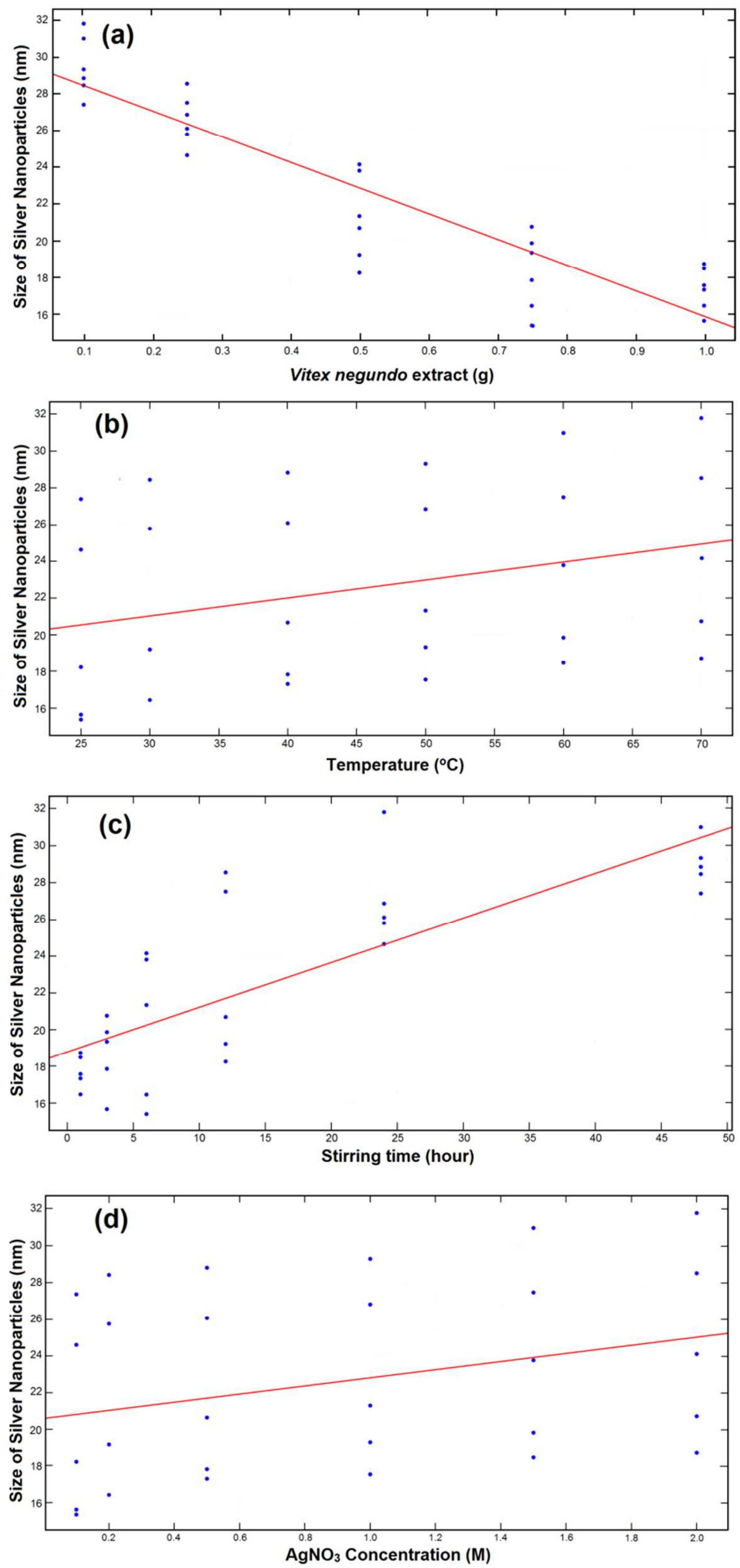

Figure 9. Two-dimensional plots, effects of amount of *V. negundo* extract (a), temperature of reaction (b), stirring time(c), $AgNO_3$ concentration on size of Ag-NPs (d).

The results were presented in Figure 9 show that measurement of size of Ag-NPs decreased rapidly with the increase in the amount of *V. negundo* extract. As inversely, increasing of temperature of reaction, stirring time, and $AgNO_3$ concentration will be increased the size of Ag-NPs.

The Figure 10 (a-f) presents the combined effects of the four input variables, on the size of nano particles. In Figure 10(a) the size of Ag-NPs on based the amount of *V. negundo* extract and temperature of reaction is presented. Indicating the points are inside the red, yellow, and dark blue areas can conclude that: "The *V. negundo* extract has the decreasing property on size of Ag-NPs and Temperature has the decreasing property" so that minimum of size of Ag-NPs is accrued in the experimental condition, 25 °C of temperature and 1.0 gram of *V. negundo* extract. Also the maximum of size of Ag-NPs outcropped in 70 °C of temperature and amount 0.2 gram of *V. negundo* extract.

The size of Ag-NPs on based the amount of *V. negundo* extract and $AgNO_3$ concentration is presented in the Figure 10(b). The points of red area show the increasing property of $AgNO_3$ concentration so that maximum of size of Ag-NPs was happened 2 mol of $AgNO_3$ concentration and 0.1 gram of *V. negundo* extract. Also the points of dark blue area indicative more effective of *V. negundo* extract on the size of nanoparticle; also they demonstrate the decreasing property of *V. negundo* extract on the measure of Ag-NPs, as the minimum of size of Ag-NPs was occurred1 gram of *V. negundo* extract and amount of less than 0.2 mol of $AgNO_3$ concentration.

The effects of concentration $AgNO_3$ and temperature of reaction on the size of nanoparticles is shown in Figure 10(c). The points of inside the green, yellow, red and dark blue areas indicate both factors are important in determining nanoparticle size. The minimum of size of Ag-NPs was befall in less than 0.2 mol of $AgNO_3$ concentration and 25 °C of temperature and also maximum of size of Ag-NPs was happened in 70 °C of temperature and amount 2 mol of $AgNO_3$ concentration.

Figure 10(d) displays the effects of stirring time and amount of temperature on output. The points inside the red and dark blue areas represents that the factor of stirring time is more important than temperature. Therefore minimum of size of Ag-NPs is happed in during less than 5 hour of stirring time and 25 °C of temperature of condition experimental, and also maximum of size of Ag-NPs is arisen in 24 hour and 60°C.

The size of Ag-NPs on based the amount of *V. negundo* extract and time of stirring is presented in Figure 10(e). The points inside of different colure of figure show factor *V. negundo* of extract is more important than stirring's time for determining nanoparticle size. Then maximum size of Ag-NPs is accrued in 24 hour of stirring time and 0.1 gram of *V. negundo* extract and minimum size of Ag-NPs is 1 hour of stirring time and 1 gram of *V. negundo* extract.

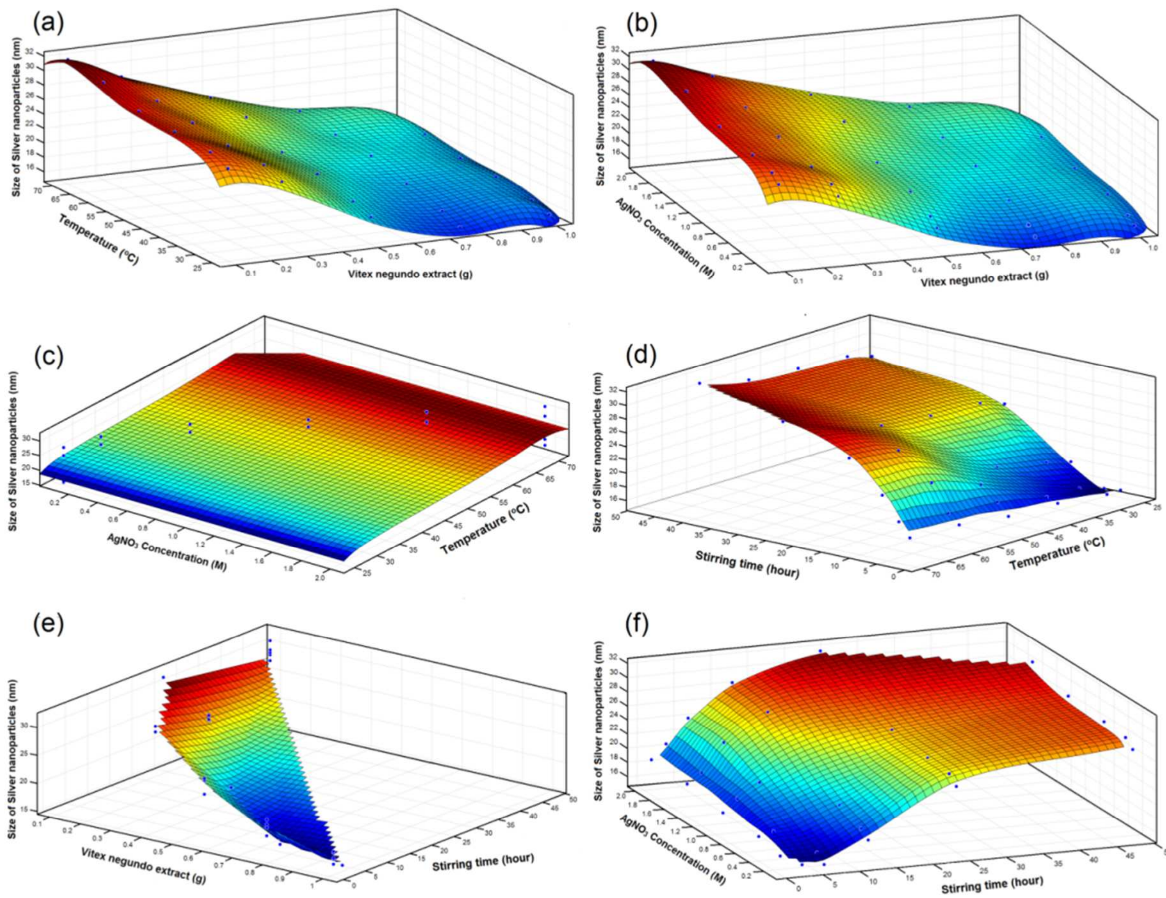

Figure 10. Three-dimensional surfaces plots shows that effect of: temperature of reaction and amount of *V. negundo* extract (a), $AgNO_3$ concentration and amount of *V. negundo* extract (b), $AgNO_3$ concentration and temperature of reaction (c), stirring time of reaction and temperature of reaction (d), amount of *V. negundo* extract and stirring time of reaction (e), and $AgNO_3$ concentration and stirring time of reaction (f) on size of Ag-NPs.

The effects of $AgNO_3$ concentration and stirring time of reaction on the size of nanoparticles are shown in Figure 10(f). The points inside the blue and yellow and orange areas demonstrate that the factor of stirring time is more important than $AgNO_3$ concentration. Therefore minimum of size of Ag-NPs is happed in during less than 5 hour of stirring time and 0.2 mol of $AgNO_3$ concentration of condition experimental, and also maximum of size of Ag-NPs is arisen in 24 hour and 2 mol of $AgNO_3$ concentration. The results obtained from Figure 10(a-f) verify the higher efficiency of amount of *V. negundo* extract compared to the other effects on the size of Ag-NPs. Also, the other important factors are stirring time, molar concentration $AgNO_3$ and reaction temperature as respectively.

Conclusion

Also in the present investigation, a neural network has been designed and demonstrated to predict the size of Ag-NPs by taking into account the effect of $AgNO_3$ molar concentration, temperature of reaction, amount of *V. negundo* extract, and stirring time of reaction. The performances of the ANN model was tested using, correlation coefficient and mean square error. The using of the suitable ANN model to predict the size of nanoparticles gives satisfactory results so that the average mean square error was 0.4576 and the correlation coefficient was 0.9982. The linear regression between size of Ag-NPs and dependent variable was applied to select the major input variables for the ANN model. Also, in this research, multiple linear regression and fitting models were used to model the impacts of numerous independent variables on the dependent variable. The experimental results demonstrated the important factors in the identity of the size of nanoparticles are as follow: amount of *V. negundo* extract, stirring time, volume of molar concentration $AgNO_3$ and reaction temperature as respectively. Then the maximum size of Ag-NPs is occurred in 60°C of temperature 24 hour of stirring time, 0.1 gram of *V. negundo* extract, and 2 mol of $AgNO_3$ concentration in the experimental condition. Also the minimum size of Ag-NPs is happened in the experimental condition as follow: 25 °C of temperature, 1 hour of stirring time, 1 gram of *V. negundo* extract, and 0.2 mol of $AgNO_3$ concentration. Therefore the proposal model can be a very efficient tool and useful alternative for the computation of production silver nanoparticles.

Acknowledgment

The authors would like to thank the Ministry of Higher Education Malaysia for funding this research project under Research University Grant Scheme No. 01G55. Also, thanks to the Research Management Center (RMC) of UTM for providing an excellent research environment in which to complete this work.

References

1. S. Iravani, *Green Chem*., 2011**, 13**, 2638-2650.

2. A. A. Kajani, A. K. Bordbar, S. H. Z. Esfahani, A. R.Khosropour, and A. Razmjou, *RSC Adv*., 2014**, 4**, 61394-61403.

3. A. K. Mittal, Y. Chisti and U. C. Banerjee, *Biotechnol. Adv*., 2013**, 31**, 346-356.

4. R. Rajan, K. Chandran, S. L. Harper, S.Yun and P. T. Kalaichelvan, *Ind. Crop. Prod.,* 2015**, 70**, 356-373.

5. H. M. M. Ibrahim, *J. Radiat. Res. Appl. Sci.,* 2015, 1-11. (dio.org/10.1016/j.jrras.2015.01.007)

6. K. Shameli, M. B. Ahmad, A. Zamanian, P. Shabanzadeh, Y. Abdollahi and M. Zargar, *Int. J. Nanomed.* 2012**, 7**, 5603-5610.

7. K. Shameli, M. B. Ahmad; P. Shabanzadeh, E. A. J. Al-Mulla, A. Zamanian, Y. Abdollahi, S. D. Jazayeri, M. Eili, F. A. Jalilian and R. Z. Haroun, *Res. Chem. Intermed.* 2014, **40** (3), 1313-1325.

8. K. Shameli, M. B. Ahmad, E. A. J. Al-Mulla, , P. Shabanzadeh, A. Rustaiyan, Y. Abdollahi, S. Bagheri, S. Abdolmohammadi, M. S. Usman and M. Zidan, *Molecules,* 2012, **17**(7), 8506-8517.

9. M. Zargar, K. Shameli, G. R. Najafi and F. *J.* Farahani, *Ind. Eng. Chem.,* 2014, **4**(20), 169-336.

10. P. Shabanzadeh, R. Yusof and K. Shameli, *J. Ind. Eng. Chem*., 2015, **24**, 42-52.

11. R. H. Nia, M. Ghaedi and A. M. Ghaedi, *J. Mol. Liq.,* 2014, **195**, 219-229.

12. A.G. Nazari and M. Mozafari, *Adv. Powder Technol.,* 2012, **23**, 220-227.

13. M. Rezakazemi, S. Razavi, T. Mohammadi, Nazari. A. G. *J. Membr. Sci.,* 2011, **379**, 214-224.

14. M. Rezakazemi and T. Mohammadi, *Int. J. Hydrogen Energ.,* 2013, **38**, 14035-14041.

15. M. Ghaedi, A. M. Ghaedi, F. Abdi, M. Roosta, R. Sahraei and A. Daneshfar, *J. Ind. Eng. Chem*., 2014, **20**, 787-795.

16. R. Hosseini Nia, M. Ghaedi and A. M. Ghaedi, *J. Mol. Liq.,* 2014, **195**, 219-229.

17. A. G. Nazari and M. Mozafari, *Adv. Powder Technol.,* 2012, **23**, 220-227.

18. M. W. Gardner and S. R. Dorling, *Proceedings* 1^{st} *International Conference on Geo Computation,* University of Leeds, UK, 1996, 359-370.

19. M. Sadrzadeh, T. Mohammadi, J. Ivakpour, N. Kasiri, *Chem. Eng. J.,* 2008**, 144**, 431-441.
20. H. Demuth and M. Beale. *Math Works*, Inc., Massachusetts, 1998.

21. P. Shabanzadeh, N. Senu, K. Shameli and M. Mohagheghtabar, *E-J. Chem.,* 2013, 305713*,* 1-8. doi.org/10.1155/2013/305713

22. D. R. Baughman, Y. A. Liu, *Academic Press*, San Diego, California, USA, 1995.

23. J. A. Freeman and D. M. Skapura, *Addison-Wesley*, Reading, Massachusetts, USA, 1992.

24. S. Haykin, *Macmillan College Co*., New York, USA, 1994.

25. P. Mehra and B. W. Wah, *IEEE Press,* Los Alamitos, California, USA, 1992.

26. X. Z. Lin, X. Teng and H. Yang, *Langmuir*, 2003, **19**, 10081-10085.

27. K. Shameli, M. B. Ahmad, E. A. J. Al-Mulla, P. Shabanzadeh and S. Bagheri, *Res. Chem. Intermed*., 2015, **41**(1), 251-263.

28. E. Farno, M. Rezakazemi,T. Mohammadi and N. Kasiri1, *POLYM. ENG. SCI.,* 2014, **54**, 215–226.

29. H. Demuth, M. Beale, *Neural Network Toolbox for Use with MATLAB, The Math-Works,* Inc., MA, 1998.

30. M. Rezakazemia, S. Razavia, T. Mohammadi and A. G.Nazarib Journal of Membrane Science, 2011, **379,** 224– 232.

31. A.P. Piotrowski, J.J. Napiorkowski, *J. Hydrology*, **476**, 97–111, doi:10.1016/j.jhydrol.2012.10.019..

32. B. Sarkar, A. Sengupta, S. De and S. DasGupta, *Separation and Purification Technology* 2009, **65,** 260–268.

33. X. Ru-Ting, H. Xing-Yuan, *RSC Advances*, 2015. *DOI: 10.1039/C5RA15109K.*

34. M. Khajeh and S. Hezaryan, *Journal of Industrial and Engineering Chemistry*, 2013, **19** 2100–2107.

35. Y. Yasin, F. B. Ahmad, M. Ghaffari-Moghaddam and M. Khajeh, *Environmental Nanotechnology,_ Monitoring & Management*, 2014,**1**, 2–7.

36. Y. Abdollahi, A. Zakaria, M. Abbasiyannejad , H. FardMasoumi , M. Ghaffarimoghaddam4 , K. Matori , H. Jahangirian and A. Keshavarziet*, Chemistry Central Journal* 2013,**7**, 96.

37. C. H. Kuo, T. A. Liu, J. H. Chen, C. M. Chang, C.J. Shieh, *Biocatalysis and Agricultural Biotechnology*, 2014, **3,** 1–6.

38. P. Shabanzadeh, N. Senu, K. Shameli and F. Ismail, *Dig. J. Nanomater. Bios.*, 2013, **8**(3), 1133-1144.

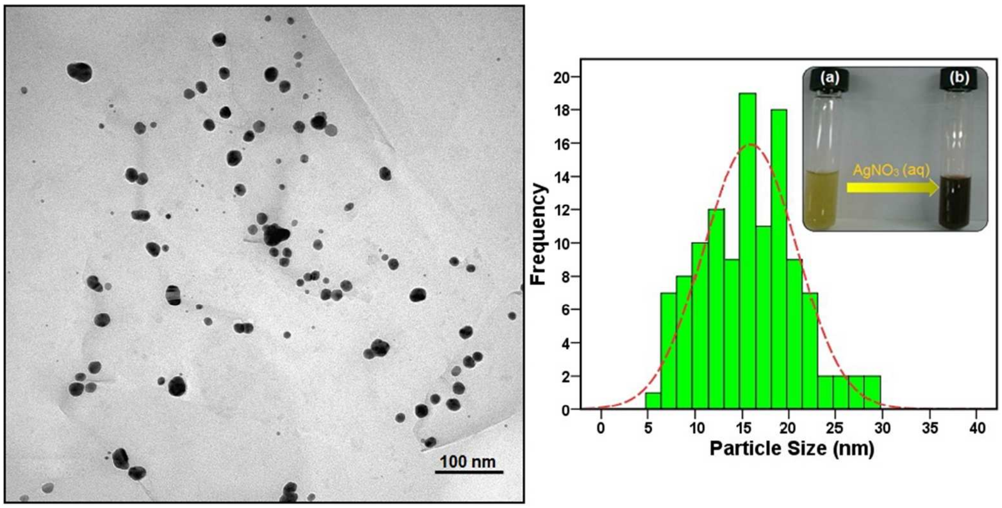

256x129mm (96 x 96 DPI)